Particle Accelerators, 1985, Vol. 17, pp. 79–107
0031-2460/85/1702–0079/$25.00/0

THE STELLATRON ACCELERATOR

C. W. ROBERSON

Office of Naval Research, Arlington, VA 22217 U.S.A.

A. MONDELLI

Science Applications, Inc., McLean, VA 22102 U.S.A.

and

D. CHERNIN†

Berkeley Research Associates, Springfield, VA 22150 U.S.A.

(*Received June 18, 1984; in final form September 30, 1984*)

The magnetic field configurations consisting of the combination of a weak-focusing betatron field, toroidal field and either $l = 0$ or $l = 2$ stellarator windings are assessed for their potential as focusing fields for high-current cyclic electron accelerators. These accelerators, named "stellatrons," are shown to have improved tolerance to mismatch between the average beam energy and the equilibrium beam energy that matches the vertical magnetic field compared to devices without the stellarator fields. Both analytical calculations in the paraxial approximation and numerical particle-orbit calculations are presented to substantiate this finding. The problems of orbital resonances and of injection into these devices are discussed. Earlier work in the field, much of it unpublished, is discussed and compared with the stellatron concept.

I. INTRODUCTION

Electron accelerators built to carry out nuclear and high-energy physics experiments typically carry average currents of less than an ampere at kinetic energies as high as 50 GeV. During the past twenty years, significant progress has been made in high-current, low-energy beam generation. These intense-beam accelerators are generally motivated by applications, mostly for radiation source development and for controlled nuclear fusion research. Megampere currents at megavolt energies are now routinely obtained using pulselines charged by Marx capacitor banks, connected to cold cathode (field-emission) diodes.[1]

Multikiloampere electron currents at tens of megavolts have been obtained using linear induction accelerators.[2–6] Recently, there has been considerable interest in extending the current-carrying capabilities of cyclic induction accelerators such as variations of the betatron and linear induction modules in cyclic (racetrack or other) configurations.

† Present Address: Science Applications, Inc., McLean, VA 22102 U.S.A.

Conventional betatrons[7,8] are current limited due to the defocusing effects of space charge at injection. Overcoming the space-charge limit requires high-energy injection. By injecting a beam at high energy, approximately 200 A of circulating current has been obtained in a small betatron in which the beam was ultimately accelerated to 100 MeV.[9] In another experiment using a 4-MeV induction linac, approximately 500 A of circulating current has been confined in a conventional betatron configuration.[10] Devices designed to improve the current-carrying capability of betatrons have included fixed-field alternating-gradient (FFAG) betatrons[11] and plasma betatrons.[12] The FFAG uses alternating gradient strong focusing fields[13,14] in addition to a vertical betatron field. In the FFAG, the magnetic fields remain constant in time, while the flux linking the particle orbit is changed to produce an inductive electric field. To avoid single-particle resonances as the energy is increased, the equilibrium radius of the orbit is allowed to vary with energy, keeping the orbits "self-similar". The currents achieved in prototypes[11] have been modest, limited by the tune shift due to space-charge effects.

The plasma betatron employs a toroidal magnetic field in addition to the betatron field. A plasma is injected or created in the device and the applied inductive electric field causes a portion of the electron distribution to gain more energy from the electric field between collisions than it loses during a collision, a phenomenon called electron runaway.[54] In magnetic-fusion devices, runaway currents of hundreds of amperes at energies of several MeV have been obtained.[15,16,39]

The HIPAC[17] device, using only a toroidal magnetic field with a cross-field injection scheme known as inductive charging,[18] has been investigated in connection with an ion-acceleration concept. Average electron densities of $4\times10^{9}\,\mathrm{cm}^{-3}$ have been achieved. The trapped electrons are not accelerated in this device, but are used instead to create a strong potential well for ions.

In another series of experiments,[19] average electron densities of $10^{10}\,\mathrm{cm}^{-3}$ have been achieved using inductive charging in toroidal device. A total charge of 100 microcoulombs has been trapped, which if accelerated to relativistic velocities would result in a current of 10 kA. With a time-independent vertical field and a transformer used to produce an inductive electric field, only small electron current ($<$50 A) is obtained. The results indicate that the electric cloud is not accelerated, but remains trapped in the torus.

Current interest has been focused on high-current nonneutral electron-beam acceleration.[20] Recently, a modified betatron configuration has been suggested[21–23] that employs a conventional weak-focusing betatron field and toroidal magnetic field. The principal advantage offered by the modified betatron is that the toroidal magnetic field reduces the required injection energy by containing the space-charge defocusing forces. Extensive analysis of this configuration has been carried out both analytically and numerically.[24–34]

Recent experiments employing inductive charging in a modified betatron configuration have achieved beam currents of approximately 200 A and energies of approximately 1 MeV using 30-kV injection voltage.[35] In an elongated or "stretched" modified betatron, beam currents of approximately 50 A at energies of 1 MeV have been achieved using 50-kV injection.[34]

Another approach to high-current cyclic accelerators is the use of linear induction modules in a cyclic configuration. One such scheme[3] has used a long-pulse linear induction module with beam recirculation through isolated beam paths for each transit through the induction module.[36] This configuration is essentially a folded induction linac. Yet another approach is to use a long-pulse induction module in a racetrack geometry. High currents can be handled by adding a toroidal magnetic field. This field introduces particle drifts in the bends, however, which can be averaged out by the addition of stellarator windings.[37] For reasonable parameters, the stellarator windings can contain particles with energies up to approximately 1 MeV per kilogauss of stellerator field on a 1-m radius of curvature bend,[38] based on single-particle numerical orbit integrations.

If a time-dependent vertical magnetic field is added to the bends in order to guide the beam, then the stellerator windings provide bandwidth for an energy mismatch between the beam energy and the matched energy in the vertical field. The matched energy in the vertical magnetic field is approximately 30 MeV/kG-m.[38]

The bandwidth can be important, not only because it allows one to handle beams with a significant variation in kinetic energy, but also because it reduces the sensitivity of the system to abrupt changes such as occur at accelerating gaps.

This paper describes an analysis of a configuration consisting of a combination of stellarator and betatron fields, called the stellatron.[40–43] The motivation, in part, has been to increase the allowed mismatch between the beam energy and the betatron field. In both the conventional and modified betatron, the allowed mismatch $\Delta\gamma/\gamma_0$ is given by

$$\frac{\Delta\gamma}{\gamma_0} \leq \tfrac{1}{2}(1-n)\frac{a}{r_0},$$

where n is the betatron field index and a/r_0 is the inverse aspect ratio of the accelerator chamber. Typically $a/r_0 = 0.1$ and so $\Delta\gamma/\gamma_0 \leq 2.5\%$ is the allowed bandwidth for mismatch in the conventional and modified betatron for $n = 1/2$. Since the vertical field at injection in several planned experiments is generally less than 100 G, field errors of a few gauss can cause loss of the beam.

By adding a stellarator field to a cyclic accelerator, a strong-focusing system is obtained that can sustain high currents and large mismatch between particle energy and vertical field. Stellarator fields are most simply characterized by two integers, l and m, these being respectively the number of field periods in the poloidal and toroidal directions in the device [see Eq. (3) and Fig. 3A below]. Two special cases have been treated in some detail. The $l = 2$ stellatron[40,41] is shown in Fig. 1. The stellarator field consists of a toroidal field plus a continuously twisted quadrupole field. The twisted quadrupole configuration is analogous to the alternating-gradient strong-focusing fields that are routinely utilized in modern synchrotrons.

The $l = 0$ stellatron shown in Fig. 2 is similar to a bumpy-torus fusion device with the addition of the betatron field. Here, the varying radial-field component leads to strong focusing. The $l = 1$ configuration has no transverse field gradient at the beam axis, and therefore is only weakly focused. Stellatrons with $l \geq 3$ are

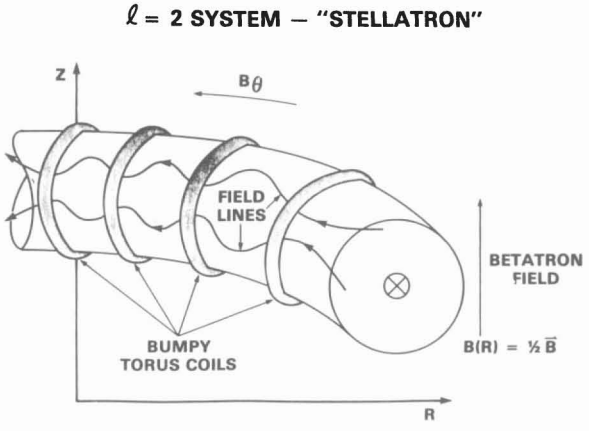

FIGURE 1 The $l = 2$ stellatron.

high-shear devices with low fields near the magnetic axis. The nonlinear properties of these configurations may be useful in conjunction with $l = 0$ or $l = 2$ focusing fields to provide detuning of orbital resonances.

In Section II, the stability properties of the $l = 0$ and $l = 2$ configurations are derived, including the effects of the self fields of the beam. The particle tunes are calculated. In Section III particle orbits for the conventional and modified betatrons and the $l = 0$ and 2 stellatrons are calculated numerically and compared. The energy-mismatch bandwidth of the stellatron is calculated as a function of the focusing strength. The sensitivity of the particle orbits to the betatron field index in the stellatron is also examined.

In Section IV, integer orbital resonances in the stellatrons are discussed. Integer orbital resonances occur when the betatron "tune" (the number of betatron wavelengths around the circumference) is an integer. In Section V, various

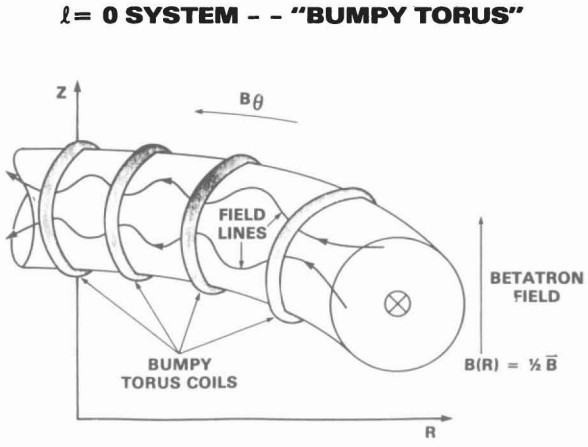

FIGURE 2 The $l = 0$ stellatron.

high-current injection schemes are described and the potential advantages offered by the stellatron are examined. Section VI is a discussion of the available literature (much of it unpublished), and Section VII presents a summary of the results.

II. PARTICLE ORBITS IN THE PARAXIAL APPROXIMATION

A linearized or paraxial analysis of particle orbits, valid for a particle that is "near" a circular design orbit with "nearly" the correct energy to be matched on that orbit, has been carried out to gain some quantitative understanding of particle behavior in the stellatron. Orbits of particles not satisfying these conditions must in general be found numerically, as discussed in the following section. The linearized analysis, however, yields important information about the frequency and the stability of the particle oscillations about the design orbit.

The analysis employs a general magnetic-field configuration which we describe in the coordinates of Fig. 3A. The applied fields consist, in part, of a vertical and radial "betatron" field of the form

$$\mathbf{B}^b \approx -\frac{nz}{r_0} B_{z0}\hat{r} + B_{z0}\left[1-\frac{n(r-r_0)}{r_0}\right]\hat{z}, \tag{1}$$

where $(r, z) = (r_0, 0)$ is the location of the design orbit (assumed circular), B_{z0} is the vertical field at the design orbit, and n is the betatron field index. A toroidal field,

$$B_{\theta 0}\left[1-\frac{r-r_0}{r_0}\right]\hat{\theta}, \tag{2}$$

is superimposed on (1), as well as a "stellarator" or multipole field which is written in the cylindrical approximation as the negative gradient of the scalar potential

$$\Phi^s(\rho, \phi, s) = -\frac{B_{s0}}{k} 2^l I_l(k\rho) \sin(l\phi + ks), \tag{3}$$

where $k = m/r_0$ and B_{s0} are constants and l and m, referred to as the poloidal and toroidal field numbers respectively, are taken as integers. In addition, s is defined to be $-r_0\theta$, so that (ρ, ϕ, s) is a righthanded system. The axis of the stellarator field is assumed to be aligned with the symmetry plane of the betatron field, $z = 0$.

Each of the fields (1)–(3) has its own special purpose. The betatron field (1), of course, acts simply to cancel the centrifugal force experienced by a circulating particle. In a stellatron, this field rises with the particle energy so that the betatron condition is (at least approximately) satisfied. The weak-focusing nature of (1), when n is between 0 and 1, which is crucial to the successful operation of betatrons, is of secondary importance to the stellatron. Stable orbits still occur in the stellatron when n is outside of the interval (0, 1). The stellatron configuration therefore has the virtue of being insensitive to errors in the vertical field or its gradient. This insensitivity has beneficial consequences in practical designs.

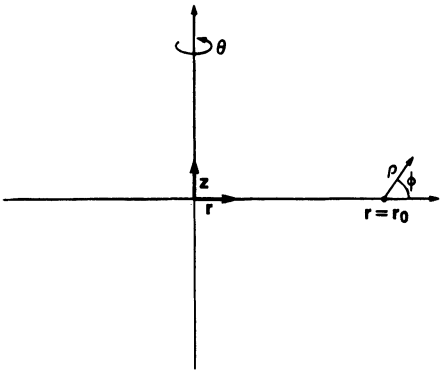

Fig. 3A

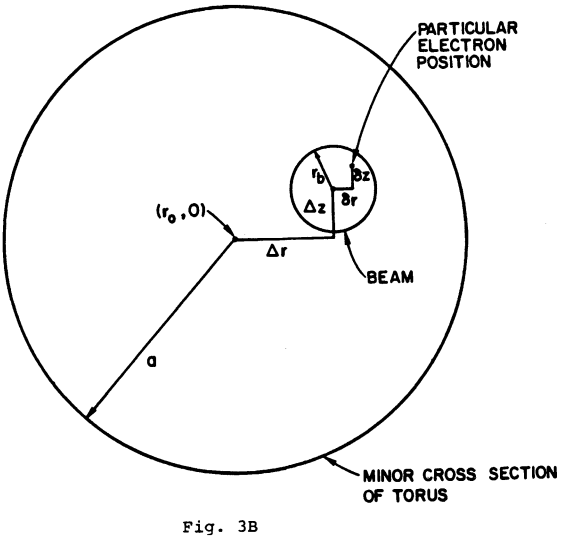

Fig. 3B

FIGURE 3 Geometry and coordinate systems. The origin in Fig. 3A is at the center of a torus of major radius r_0. Fig. 3B illustrates a cut along the minor cross section, showing the beam and individual particle positions.

A toroidal field (2) is added to the conventional betatron in the hope of increasing the contained current. Indeed, it has been found that with only fields (1) and (2) the beam densities which can be contained in equilibrium increase by a factor $(B_\theta/2B_z)^2$, for large B_θ, over those in a conventional betatron, (1). Additionally, the toroidal field acts to control the tune shift due to the effects of space charge. This feature is important when orbital resonances must be avoided.

The stellarator field (3) is added to provide the beneficial effects of alternating-gradient strong focusing. For $l = 0$ or 2, Eq. (3) gives an alternating gradient field component at the design orbit. This field greatly improves the momentum compaction over that of a configuration consisting of (1) and (2) only, and so

greatly relaxes certain design tolerances of the machine. Windings of other l-number may also be useful; in particular fields with $l \geq 3$ may help in controlling orbital resonances, but the analysis must be done numerically. The $l = 1$ field produces an oscillating magnetic field (not a field gradient) on the axis; such a configuration would not possess a circular design orbit and is not expected to possess any noteworthy focusing properties. This paper is concerned only with stellatrons having $l = 0$ (a "bumpy torus") and $l = 2$ (a "twisted quadrupole").

Since the stellatron is intended to carry large currents, it becomes important to consider the effects of the self fields of the beam. In general, this is an extremely hard problem. To make progress analytically, a simple model for these fields is assumed, consisting of a circular beam cross section (minor radius r_b) and uniform density with center located at $(r_0 + \Delta r, \Delta z)$ in a perfectly conducting cylindrical chamber of radius a (Fig. 3B). The self fields in the stellatron at the particle location $(r_0 + \Delta r + \delta r, \Delta z + \delta z)$ are given by

$$E_r = -2\pi n_0 e\left(\delta r + \frac{r_b^2}{a^2}\Delta r\right) \tag{4a}$$

$$E_\theta = 0 \tag{4b}$$

$$E_z = -2\pi n_0 e\left(\delta z + \frac{r_b^2}{a^2}\Delta z\right) \tag{4c}$$

$$B_r = \beta_0 E_z \tag{4d}$$

$$B_\theta = 0 \tag{4e}$$

$$B_z = -\beta_0 E_r \tag{4f}$$

in cgs units, where n_0 is the beam density, $-e$ is the electron charge, and $\beta_0 = v_0/c$ is the velocity of a particle on the design orbit normalized to the speed of light. In Eqs. (4a–f), the first term in each set of parentheses is due to the self field of the beam, while the second term is due to the image of the beam in the perfectly conducting wall. Toroidal corrections to Eqs. (4) may be important in some cases but are ignored here.

l = 2 Stellatron

The case $l = 2$ is considered first in detail since this case, rather than $l = 0$, corresponds most closely to a conventional quadrupole strong-focusing system. The $l = 2$ stellarator field near the axis is, from (3)

$$\mathbf{B}^s = kB_{s0}\{[z_1 \cos m\theta - r_1 \sin m\theta]\hat{r} + [r_1 \cos m\theta + z_1 \sin m\theta]\hat{z}\}, \tag{5}$$

where $r_1 = r - r_0$, $z_1 = z$. Taking the fields (1), (2), (4), (5) and using them in the equations of motion gives equations correct to first order in the small quantities r_1/r_0, $\Delta r/r_0$, z_1/r_0, and $\Delta z/r_0$

$$\ddot{r}_1 + \Omega_{z0}^2(1 - n + \mu \cos m\theta)r_1 - \frac{1}{2}\frac{\omega_b^2}{\gamma_0^2}\left(r_1 - \Delta r + \frac{r_b^2}{a^2}\Delta r\right)$$
$$= \Omega_{z0}\gamma_0^2 v_{\theta 1} - (\mu\Omega_{z0}^2 \sin m\theta)z_1 + \Omega_{\theta 0}\dot{z}_1 \tag{6a}$$

$$\ddot{z}_1+\Omega_{z0}^2(n-\mu\cos m\theta)z_1-\frac{1}{2}\frac{\omega_b^2}{\gamma_0^2}\left(z_1-\Delta z+\frac{r_b^2}{a^2}\Delta z\right)=-(\mu\Omega_{z0}^2\sin m\theta)r_1-\Omega_{\theta 0}\dot{r}_1 \quad (6b)$$

$$\dot{v}_{\theta 1}=0, \quad (6c)$$

where $\Omega_{z0}=eB_{z0}/m_e\gamma_0 c$, $\mu=kr_0B_{s0}/B_{z0}$, $\omega_b^2=4\pi n_0e^2/m_e\gamma_0$, m_e is the electron mass, and $v_{\theta 1}=r_1\dot{\theta}_0+r_0\dot{\theta}_1$. A subscript, 0, refers to quantities evaluated on the design orbit where $v_0/r_0=\Omega_{z0}$ and dots denotes time derivatives.

As they stand, Eqs (6a–c) are not straightforward to solve since they involve both the motion of the particle about the beam center and the motion of the beam center about the design orbit. Since $r_1=\Delta r+\delta r$ and $z_1=\Delta z+\delta z$, separate solutions are required for (r_1, z_1) and $(\Delta r, \Delta z)$. A self-consistent set of equations for both beam-center motion and for motion of particles about the beam center may be found, however, by averaging (6a–b) over a distribution of particle initial conditions. Details of this averaging procedure are given in the Appendix. The result is that motion of the beam center is governed by the equations

$$\frac{\partial^2}{\partial\theta'^2}\Delta r+\left(1-n-\frac{r_b^2}{a^2}n_s+\mu\cos m\theta'\right)\Delta r=\frac{c^2}{r_0\Omega_{z0}^2}\frac{\langle\gamma_1\rangle}{\gamma_0}-(\mu\sin m\theta')\Delta z+b\frac{\partial\Delta z}{\partial\theta'} \quad (7a)$$

$$\frac{\partial^2}{\partial\theta'^2}\Delta z+\left(n-\frac{r_b^2}{a^2}n_s-\mu\cos m\theta'\right)\Delta z=-(\mu\sin m\theta')\Delta r-b\frac{\partial\Delta r}{\partial\theta'}, \quad (7b)$$

where we have changed independent variables from (θ, t) to $(\theta', t')\equiv(\theta, t-\theta/\Omega_{z0})$, i.e., Eqs. (7a–b) describe the movement of the beam center as seen by a reference particle moving with angular velocity Ω_{z0}. In Eq. (7), the notation $n_s\equiv\omega_b^2/(2\gamma_0^2\Omega_{z0}^2)$, $b\equiv B_{\theta 0}/B_{z0}$, and $\gamma_1\equiv\beta_0\gamma_0^3\beta_1$ is introduced. In Eq. (7a), the quantity $\langle\gamma_1\rangle$ is just the ensemble average of the difference in energy between a particle and the reference particle, i.e. $\langle\gamma_1\rangle\equiv\langle\gamma-\gamma_0\rangle$. $\langle\gamma_1\rangle$ is independent of time and for a matched beam, $\langle\gamma_1\rangle=0$. Once Eq. (7) is solved, the solution may be inserted into Eqs. (6a, b) which may then be solved for the location of any individual particle. The method used for solving Eq. (7) is described below, and may be used on Eq. (6) as well.

Equations (7a, b) may be completely solved in the special case $n=1/2$, a fact which traces its origin to the poloidal symmetry this value of n imposes on the restoring forces experienced by the beam. Although the solution is special in this sense, it is expected to share most of its features with the solution for arbitrary n (which must be obtained numerically) since the particle focusing should be dominated by the quadrupole strength μ and only be weakly affected by the precise value of n. For $n=1/2$, then, define the complex variable $\xi=(\Delta r+i\Delta z)/r_0$ for which Eqs. (7a, b) give the equation

$$\xi''+ib\xi'+\left(\frac{1}{2}-\frac{r_b^2}{a^2}n_s\right)\xi+\mu e^{im\theta'}\xi^*=\langle\Delta\rangle \quad (8)$$

where $\langle\Delta\rangle$ is the momentum mismatch $\langle\gamma_1\rangle/(\beta_0^2\gamma_0)$. In Eq. (8), primes denote $\partial/\partial\theta'$ and an asterisk denotes complex conjugate. The further change of variable $\xi=$

$\psi e^{im\theta'/2}$ yields an equation with constant coefficients,

$$\psi'' + i(m+b)\psi' + \left(\frac{1}{2} - \frac{r_b^2}{a^2} n_s - \frac{mb}{2} - \frac{m^2}{4}\right)\psi + \mu\psi^* = \Delta e^{-im\theta'/2}, \tag{9}$$

the solution to which consists of a particular solution plus a sum of exponentials of the form $\psi_0 e^{\pm i\nu_\pm \theta'}$ where ψ_0 is a constant and $\nu_\pm$ are given by

$$\nu_\pm = [\hat{n} + \tfrac{1}{4}\hat{m}^2 \pm (\hat{n}\hat{m}^2 + \mu^2)^{1/2}]^{1/2}, \tag{10}$$

where $\hat{n} = 1/2 - r^2/a^2 n_s + b^2/4$, $\hat{m} = m + b$. A particular solution to Eq. (9) is

$$\psi_p = Ae^{im\theta'/2} + Be^{-im\theta'/2}, \tag{11}$$

where

$$A = \frac{\mu\langle\Delta\rangle}{\left[m^2 + mb - \frac{1}{2} + \frac{r_b^2}{a^2} n_s\right]\left[\frac{1}{2} - \frac{r_b^2}{a^2} n_s\right] + \mu^2} \tag{12}$$

$$B = \frac{\langle\Delta\rangle}{\frac{1}{2} - \frac{r_b^2}{a^2} n_s + \mu^2\left[m^2 + mb - \frac{1}{2} + \frac{r_b^2}{a^2} n_s\right]^{-1}}. \tag{13}$$

Referring back to the definitions of ξ and ψ, it is evident that B gives the "zero-frequency" part of the radial shift due to a beam with momentum mismatch $\langle\Delta\rangle$, that is, $B/\langle\Delta\rangle$ is the momentum compaction factor, which may be made small by choosing μ large. Setting $\mu = 0$ in Eq. (13) recovers the usual result for a conventional betatron or modified betatron. (Addition of a toroidal field to a conventional betatron does not affect momentum compaction.)

The small oscillations of the beam center are stable ($\nu_\pm$ are real) if and only if three conditions are satisfied

$$\hat{n} + \tfrac{1}{4}\hat{m}^2 > 0 \tag{14a}$$

$$(\hat{n} - \tfrac{1}{4}\hat{m}^2)^2 - \mu^2 > 0 \tag{14b}$$

$$\hat{n}\hat{m}^2 + \mu^2 > 0. \tag{14c}$$

These conditions are summarized in Fig. 4, where the stable region of parameter space is illustrated in terms of the auxiliary variables $u = 4\hat{n}/\hat{m}^2$ and $v = |\mu|/\hat{m}^2$. Typically one operates in the stable region with $u < 1$. The orbital stability requirement places strict limits on the size of μ that can be tolerated, i.e., strict limits on the achievable momentum compaction for given b and m. Any experiment must be designed so that u and v remain in the stable region for all time; a sample experimental trajectory is illustrated in the figure. For a low current beam $\hat{n}$ is positive and Eq. (14b) gives the only nontrivial condition

$$|\tfrac{1}{2}m^2 + mb - 1| > |2\mu| \tag{15}$$

The orbital stability criteria for individual particle motion within the beam are of identical form to Eqs. (14a–c) with the replacement, in the definition of $\hat{n}$, of

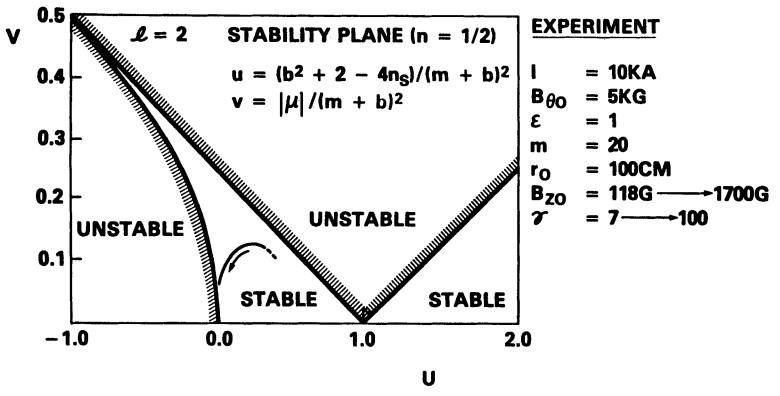

FIGURE 4 The $l = 2$ stability plane. u and v are defined in the text. The arrow indicates a sample experimental trajectory.

$(r_b/a)^2 n_s \to n_s$. That this is so may be seen by an analysis of Eqs. (6a, b) exactly parallel to that carried out for Eqs. (7a, b) considering that now, in Eqs. (6a, b), Δr and Δz are known quantities. With this substitution in Eq. (13), the zero-frequency term in the individual particle motion is obtained as

$$B_p = \frac{\Delta - \langle \Delta \rangle}{\frac{1}{2} - n_s + \mu^2 (m^2 + mb - \frac{1}{2} + n_s)^{-1}}, \tag{16}$$

where $\Delta = \gamma_1/\gamma_0\beta_0^2$ is proportional to the energy difference between the individual electron energy and the matched beam energy. With $\mu = 0$, the results for a conventional betatron and a modified betatron are obtained. This solution with $\mu = 0$ suffers a loss of momentum compaction, i.e., $B_p \to \infty$, when n_s passes through 1/2. In a conventional betatron, $n_s \leq 1/2$ is required for orbital stability. The modified betatron, however, would typically use $n_s \gg 1/2$ at injection, and would then pass through $n_s = 1/2$ during acceleration, since $n_s \propto \gamma^{-3}$. This transition at $n_s = 1/2$ corresponds to a momentary loss of equilibrium in the modified betatron as the configuration switches from a diamagnetic to a paramagnetic equilibrium.[26,27]

This transition can be avoided in the stellatron by using large $|\mu|$. The stability condition (14b), however, sets an upper limit to $|\mu|$ for a particular choice of m, b and n_s. The requirement on μ^2 may be expressed as

$$(n_s - 1/2)(m^2 + mb + n_s - 1/2) < \mu^2 < (n_s - 1/2 + m^2/4 + mb/2)^2. \tag{17}$$

For the condition (17) to be meaningful, n_s must satisfy

$$n_s - \frac{1}{2} < \frac{1}{2}\left(\frac{m}{2} + b\right)^2, \tag{18}$$

which is clearly compatible with $n_s \gg 1/2$. The $l = 2$ stellatron, therefore, can avoid a loss of momentum compaction during acceleration, while retaining the ability to use large n_s at injection.

$l = 0$ Stellatron

The $l = 0$ stellatron has fields given by

$$B_r^s \simeq \tfrac{1}{2} B_{s0} m x \sin m\theta \tag{19a}$$

$$B_\theta^s \simeq B_{s0} \cos m\theta \tag{19b}$$

$$B_z^s \simeq \tfrac{1}{2} B_{s0} m y \sin m\theta \tag{19c}$$

in a cylindrical (r, θ, z) coordinate system (Fig. 3), where $x = r_1/r_0$ and $y = z_1/r_0$. Using the procedure described above for linearizing the equations of motion in the displacement from a reference orbit and using the paraxial approximation for the electron motion with $n = 1/2$, the equations of motion for single electrons including beam self-fields may be expressed as

$$\psi'' + \frac{1}{m^2}[2 - 4n_s + b^2(1 + \varepsilon \cos 2\theta_m)^2]\psi = \frac{4}{m^2}\frac{\delta P}{P_0} \exp\left[\frac{ib}{2m}(2\theta_m + \varepsilon \sin 2\theta_m)\right], \tag{20}$$

where $\varepsilon = B_{s0}/B_{\theta 0}$, $\theta_m = m\theta/2$, P_0 is the momentum of a particle which is matched on the reference orbit, δP is the "momentum error", and

$$\psi = (x + iy) \exp\left[\frac{i}{2}\int b(1 + \varepsilon \cos m\theta)\, d\theta\right]. \tag{21}$$

In Eq. (20), n_s will in general depend on θ in a way governed by an envelope equation, thereby making the inclusion of self-field effects more difficult than for the $l = 2$ case in which a constant beam radius can be maintained.[57] Consequently, only single-particle orbits will be considered.

Equation (20) is a Hill equation, for which there are theorems concerning characteristic frequencies and stability.[44] The Floquet solutions to this equation for $n_s = 0$, are of the general form

$$\psi = e^{i\nu\theta m} \sum_{n=-\infty}^{\infty} C_n e^{i2n\theta_m}, \tag{22}$$

which display an infinite set of natural oscillations at the frequencies, $\nu \pm 2n$. The value of ν can be determined numerically for a given set of accelerator parameters, but the dependence of ν on these parameters is not known analytically.

It is possible to determine and display the regions of parameter space where ν is real, i.e., where the motion is stable. Starting with the homogeneous equation,

$$\psi'' + \frac{1}{m^2}[2 + b^2(1 + \varepsilon \cos 2\theta_m)^2]\psi = 0, \tag{23}$$

the solution $\psi(\pi)$, which satisfies $\psi(0) = 1$ and $\psi(0) = 0$ is constructed numerically. The stability condition[44] is $|\psi(\pi)| < 1$, which is illustrated in Fig. 5 for a particular example. The intersections of the unstable regions with the abscissa are given by

$$\frac{1}{m^2}(b^2 + 2) = q^2; \qquad q = 1, 2, \ldots \tag{24}$$

which correspond to resonances between the "focusing frequency" which a

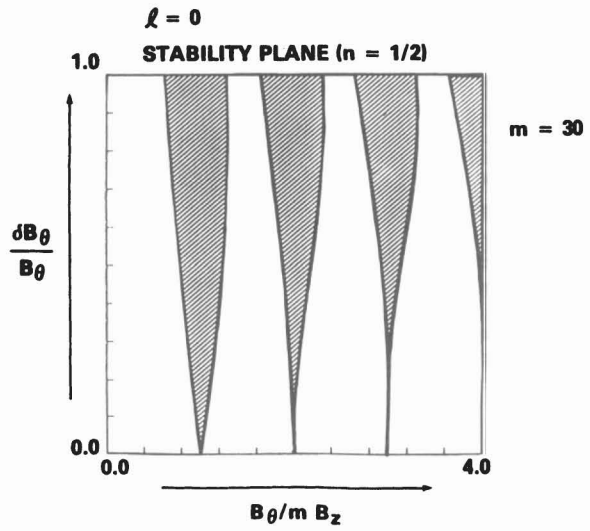

FIGURE 5 The $l = 0$ stability plane. The shaded regions are unstable.

particle experiences and its cyclotron frequency in the toroidal field. Under resonant conditions, there is a transfer of energy from longitudinal to transverse motion and the adiabatic invariance of the magnetic moment in the toroidal field is destroyed. During acceleration, if B_z is increased and B_θ is held fixed, the operating point on Fig. 5 will move from right to left. The accelerator should operate in the left-most stable band to avoid crossing unstable bands. At injection, therefore, $m > b$ is required, which implies the need for a large number of field periods. When space-charge effects are taken into account, one finds the stronger requirement, $m > 2b$, to avoid envelope instabilities.[64]

The momentum compaction factor for the $l = 0$ configuration may be calculated, for small values of ε and b/m, directly from Eq. (20). For $n_s = 0$, the result is

$$\frac{\delta x}{(\delta p/p_0)} = 2\left[1 - \left(\frac{\varepsilon b}{2}\right)^2 \frac{1}{1-(b/m)^2}\right] \tag{25}$$

which illustrates the helpful effect of the alternating gradient, as measured by ε, on the tolerance of the $l = 0$ device to momentum mismatch. When ε or b/m is large, numerical integration of the orbit equations is required.

III. NUMERICAL CALCULATION OF SINGLE-PARTICLE ORBITS

A computer code, which integrates the single-particle equations of motion, has been utilized to study nonlinear aspects of the stellatron configuration. The code solves the fully relativistic dynamical equations, without utilizing the paraxial

approximation for the electron motion or an expansion in the particle displacement from a reference orbit. The applied fields in the code include toroidal corrections to first order in the inverse aspect ratio. In addition, the code does not assume the field index to be 1/2.

The total magnetic field used by the code is the superposition of a conventional betatron field B_b and a stellarator field B_s. The conventional betatron field is given in Eq. (1). The stellarator field may be expressed as

$$\mathbf{B}_s = -\nabla\Phi_s \tag{26}$$

where ϕ_s is the magnetic scalar potential for the stellarator field. To first order in the inverse aspect ratio, ϕ_s has been given by Danilkin[45] as

$$\begin{aligned}\Phi_s(\rho, \phi, s) = -B_{\theta 0}\Bigg\{ & s + \frac{\varepsilon_1}{\alpha} I_l(x) \sin[l\phi - l\alpha s] \\ & - \frac{\kappa\varepsilon_l}{4l\alpha^2}[x^2 I_l'(x) - x(1+l)I_l(x)] \sin[(l+1)\phi - l\alpha s] \\ & - \frac{\kappa\varepsilon_l}{4l\alpha^2}[x^2 I_l'(x) - x(1-l)I_l(x) \sin[(l-1)\phi - l\alpha s] \\ & + \frac{\kappa\varepsilon_l}{4l\alpha^2}\left[\frac{K_{l+1}(x_0) - x_0 K_{l+1}'(x_0)}{K_l'(x_0)} + x_0^2\right] I_{l+1}(x) \sin[(l+1)\phi - l\alpha s] \\ & + \frac{\kappa\varepsilon_l}{4l\alpha^2}\left[\frac{K_{l-1}(x_0) - x_0 K_{l-1}(x_0)}{K_l'(x_0)} + x_0^2\right] I_{l-1}(x) \sin[(l-1)\phi - l\alpha s]\Bigg\},\end{aligned} \tag{27}$$

where $s = r_0\theta$, $x = l\alpha\rho$, $\alpha = 2\pi/L$, L is the helix pitch length, $\kappa = 1/r_0$, $x_0 = l\alpha\rho_c$, $\rho = \rho_c$ is the location of (assumed) wall surface currents, and I, K are the modified Bessel functions. The coordinates, (ρ, ϕ, s) are defined in Fig. 3. More generally, the field may be expressed as a superposition of fields of different l-number. This feature has not been included in the numerical model. In addition, beam image forces may be included in the model, but have not been utilized for any of the results presented in this section. The wave number, $k = m/r_0$, in the preceding analytical model is equivalent to $-l\alpha$.

Figure 6 shows single-particle orbits obtained with this code. The figure is the projection of the orbits onto the minor cross-section. The torus has a $1m$ major radius and $0.1m$ minor radius. The vertical magnetic field is fixed at $B_{z0} = 118$ G, corresponding to a matched particle (at the minor axis) with $\gamma_0 = 7$. The individual frames of Fig. 6 show a comparison of particle orbits in a conventional betatron, a modified betatron, an $l = 0$ stellatron and an $l = 2$ stellatron. Each frame shows two particle trajectories, one with positive mismatch and one with negative mismatch. All the trajectories are initialized on the minor axis with momentum parallel to the minor axis, and with various amounts of energy mismatch, $\Delta\gamma/\gamma_0$, as shown under each frame. The conventional and modified betatron frames demonstrate that these devices cannot tolerate mismatch, $\Delta\gamma/\gamma_0 = \pm 3\%$. In fact, using Eq. (12), we can estimate the tolerance of these devices to energy mismatch.

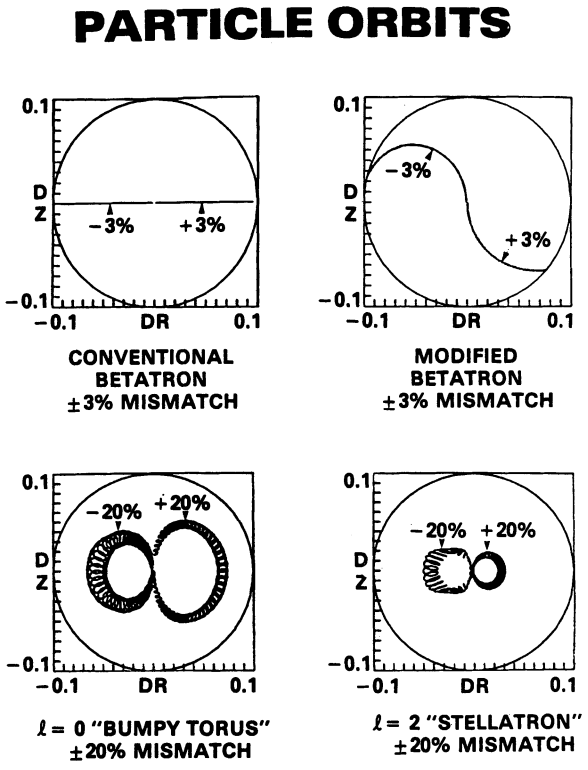

FIGURE 6 Particle orbits in conventional betatron, modified betatron, $l=0$ stellatron, and $l=2$ stellatron.

For $n_s(r_b/a)^2 \ll 1/2$, the allowed energy mismatch is given by

$$\frac{\Delta\gamma}{\gamma_0} \leq \frac{1}{4}\frac{a}{r_0}. \tag{28}$$

For $a/r_0 = 0.1$, we obtain $\Delta\gamma/\gamma_0 \leq 2.5\%$, which is consistent with the figure. The $l=0$ and $l=2$ stellatron configurations, on the other hand, can retain particles with more than $\Delta\gamma/\gamma_0 = \pm 20\%$ mismatch, as shown on the lower two frames of Fig. 6.

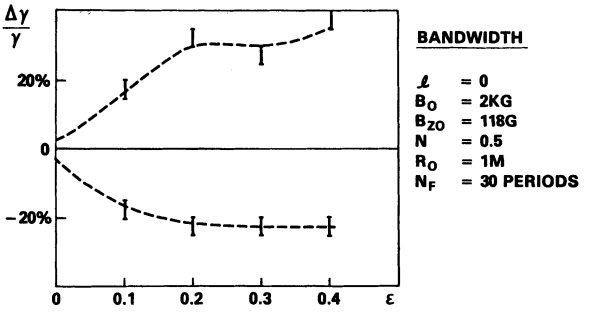

FIGURE 7 Energy bandwidth as a function of focusing strength ε for the $l=0$ stellatron. ($n = 1/2$).

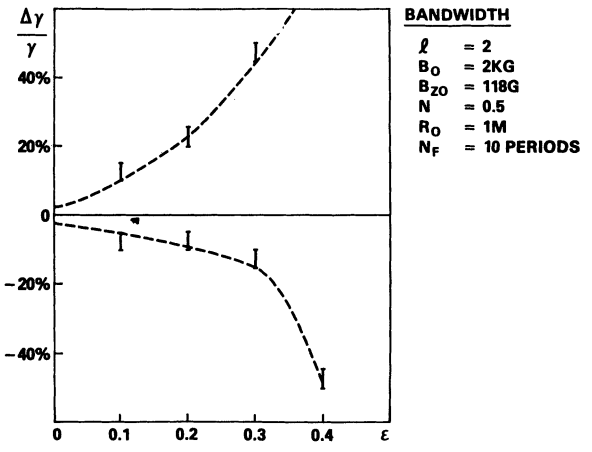

FIGURE 8 Energy bandwidth as a function of focusing strength ε for the $l = 2$ stellatron. ($n = 1/2$).

The tolerance of the accelerator to mismatch between the average beam energy and the vertical magnetic field can be described as a bandwidth of allowed mismatch. For larger mismatch, the beam excursion from its reference orbit does not fit inside the accelerator aperture. The bandwidth, therefore, is essentially a measure of the momentum compaction of the accelerator. Since a calculation of the bandwidth involves particles with large $\Delta\gamma/\gamma_0$ that make large excursions from the reference orbit, the analytical formalism of the preceding section is inadequate.

By launching particles as shown in Fig. 6, with various $\Delta\gamma/\gamma_0$, the largest $|\Delta\gamma/\gamma_0|$ for which the particle is contained can be found. This bandwidth can be displayed as a function of any parameter of the accelerator. Figures 7 and 8, for example, show the bandwidth for the $l = 0$ and $l = 2$ stellatrons as the amplitude of the

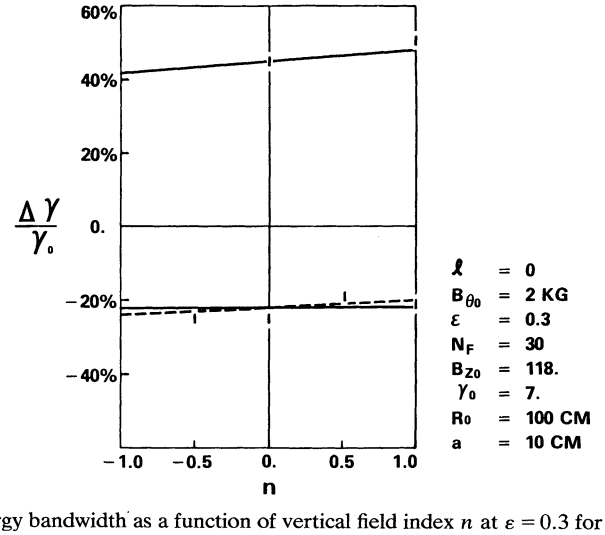

FIGURE 9 Energy bandwidth as a function of vertical field index n at $\varepsilon = 0.3$ for the $l = 0$ stellatron.

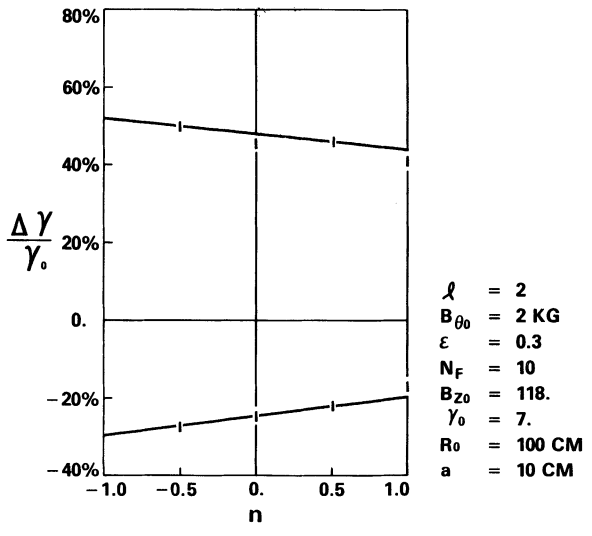

FIGURE 10 Energy bandwidth as a function of vertical field index n at $\varepsilon = 0.3$ for the $l = 2$ stellatron.

strong focusing field is varied. In both devices, the bandwidth is ±2.5% in the limit where $\varepsilon = 0$, and exceeds 20% for $\varepsilon > 0.3$. For $l = 2$, the quantity, μ, in the preceding section is given by $\mu = \varepsilon mb/2$, where $b = B_{\theta 0}/B_{z0}$.

Figures 9 and 10 show the bandwidth for the $l = 0$ and $l = 2$ stellatrons at $\varepsilon = 0.3$ as the vertical field index is varied. The results here demonstrate the relative insensitivity of the stellatron configurations to the field index. The need to maintain good uniformity in the field index for a conventional or modified betatron drives the stored energy and cost for the vertical field coils (or leads to the use of iron) in those accelerators. The stellatron configuration greatly relaxes the need for such uniformity.

IV. ORBITAL RESONANCES IN THE STELLATRON

Until now, the applied fields in the stellatron have been assumed to be "perfect" in the sense that only the fields described analytically above in Eqs. (1–3) are present. In general, of course, a physical magnet system will have some imperfections leading to small field and focusing errors, which can be represented by additional terms in the paraxial equations. Generally these small errors lead to a small response but under certain conditions—when some rational number of particle wavelengths fit around the machine—the particle orbits can be violently disrupted. In this section, these resonance conditions are considered for the $l = 0$ and $l = 2$ stellatrons, and possible ways either to avoid them or to minimize their effects are discussed. It must be said however, that there is no reason why such resonances should be of any less concern in the modified betatron and stellatron class of devices than they are in more conventional cyclic accelerators in which

they are of course, of crucial importance in establishing an operating point. Though some of the high mode-number integer resonances might be successfully passed through, there is considerable reason to believe that major beam disruptions may occur at low-order resonance crossings, if such are attempted. This point is not often sufficiently stressed in the literature promoting the use of devices similar to some of those employed in magnetic-confinement fusion research to accelerate large currents to high energies.

This section will focus on the integer resonances, driven by the Fourier components of an error in the vertical field, though others may also be important. The tune shift due to space charge will also be neglected at first, to consider the resonant response of single particles.

As in the previous section, the $l = 2$ case, for which the tunes may be explicitly calculated [Eq. (10)], is considered first. For single-particle motion, the four possible "betatron" frequencies are $m/2 \pm \nu_{\pm}$ where $\nu_{\pm}$ satisfies the biquadratic,

$$\nu^4 - (\tfrac{1}{2}m^2 + mb + b^2 + 1)\nu^2 + \tfrac{1}{4}(\tfrac{1}{2}m^2 + mb - 1)^2 - \mu^2 = 0. \tag{29}$$

The most general resonance condition is written

$$n_1\left(\frac{m}{2} + \nu_+\right) + n_2\left(\frac{m}{2} - \nu_+\right) + n_3\left(\frac{m}{2} + \nu_-\right) + n_4\left(\frac{m}{2} - \nu_-\right) = p, \tag{30}$$

where $n_1, \ldots, n_4$, p are all integers; this condition applies to all types of resonant driving terms. Integer resonances occur when all n_j except one, n_k, vanish and $p/n_k = n$ is itself an integer, the Fourier mode number of the field error. When an integer resonance occurs, the displacements which a particle undergoes on successive encounters with a field "bump" add in phase and the result can be loss of the particle from the machine.

Figure 11 shows the integer resonance contours $1, 2, \ldots, 10$ in the $b - \mu$ plane for $m = 20$. (The n and $m - n$ contours coincide.) The resonance contours are all hyperbolae, from Eq. (29); the stability boundary coincides with the degenerate case $n = m/2$. Ideally, an accelerator should be designed to avoid all resonance contours, a design which may clearly be realized by holding b and μ fixed during acceleration (neglecting the tune shift due to space charge, which may, in fact, limit the current in this as in other cyclic devices). If b and μ are allowed to change during acceleration, it may be possible to pass through at least some of the integer resonances, though this is only speculation based on a few computer studies. The possibility of passing through resonances in the stellatron is discussed further below.

The resonance situation in the bumpy torus is somewhat less straightforward to analyze. In the presence of an error in the vertical field having Fourier mode number k, a term of the form

$$(\text{const}) \cdot \exp\left[2ik\theta_m/m + (ib/2m)(2\theta_m + \varepsilon \sin 2\theta_m)\right] \tag{31}$$

is added to the right-hand side of Eq. (23), where the multiplicative constant is proportional to the magnitude of the field error. One may employ the Green's function constructed from the Floquet solutions to Eq. (23) to deduce that a

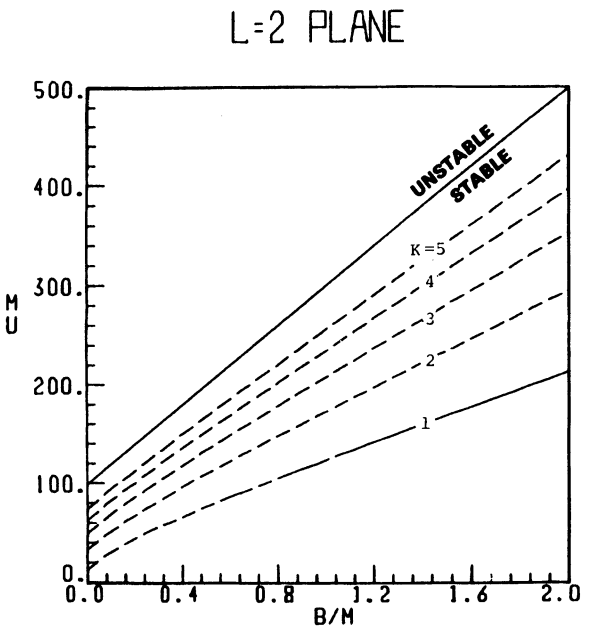

FIGURE 11 Integer-resonance contours in the $b/m - \mu$ plane for the $l = 2$ stellatron.

secular term, proportional to θ_m, will occur in the particular solution if

$$\cos \pi\left(\frac{b+2k}{m}\right) = \psi_1(\pi), \tag{32}$$

where ψ_1 is the solution to the homogeneous equation satisfying $\psi_1(0) = 1$, $\psi_1'(0) = 0$. Contours along which Eq. (32) is satisfied may be generated numerically for each k in the $b/m - \varepsilon$ plane; an example is shown in Fig. 12. Note the behavior of the $k = 0$ resonance line, which crosses other k-lines at $b/m = 2 - k/m$ in the second stable band. A $k = 0$ field error is equivalent to a momentum error, so one expects momentum compaction to be poor near the $k = 0$ contour. It is unlikely, however, that one would try to operate in the second stable band.

It is clear that the "stable" regions of Fig. 12 are in fact criss-crossed with potentially dangerous resonance lines which must either be avoided or crossed somehow during the course of an experiment. The operating point of an accelerator may be held fixed in the plane, of course, by raising all fields in synchronism, i.e., by keeping $\varepsilon = \delta B_\theta / B_{\theta 0}$ and $b = B_{\theta 0}/B_{z0}$ fixed for all time. It is worth considering the feasibility of crossing these resonances, however, since increasing all the fields together has definite large costs in terms of field energy. It might be desirable, for instance, to accelerate while keeping $B_{\theta 0}$ and $\delta B_{\theta 0}$ fixed in time, allowing the tunes to change as b does. The immediate question is, "can resonances be passed through without major disruption of the beam?"

Since resonances occur when the number of betatron wavelengths completed in one major revolution (i.e., the "tune") is an integer, half-integer, or other rational

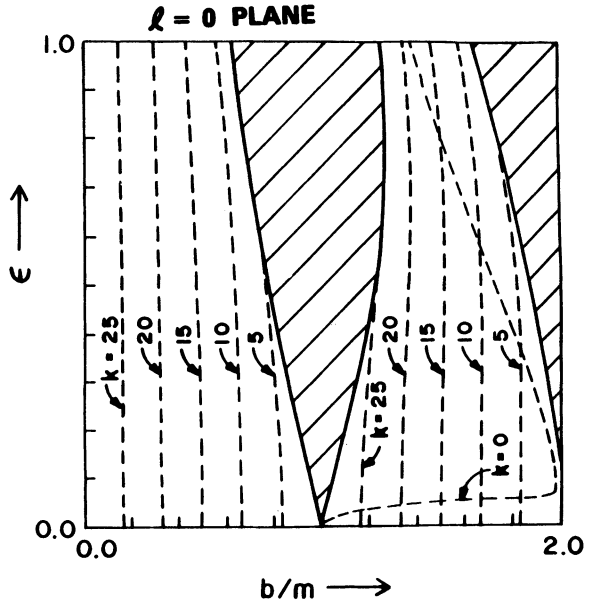

FIGURE 12 Integer-resonance contours in the $b/m - \varepsilon$ plane for the $l = 0$ stellatron.

number, a possible solution may consisting of setting constant tune by allowing the particle reference orbit to have a variable major radius (i.e., to be noncircular). The FFAG accelerator works in this fashion, and achieves constant tunes by forcing "self-similar" orbits during acceleration. A conventional betatron is the special case where the self-similar orbits also have constant radius. With addition of a toroidal field which varies as r^{-1}, however, there is no nonsynchronous field solution with constant tune, as shown below.

The single-particle tunes ($n_s = 0$) in a stellatron depend on the poloidal and toroidal field numbers (l and m), which are assumed fixed, as well as on the field ratios, $b = B_{\theta 0}/B_{z0}$ and $\varepsilon = B_{s0}/B_{\theta 0}$, at the reference orbit. In a modified betatron, the tunes depend only on b. The B_θ and B_z fields have the assumed dependence

$$B_\theta = B_{\theta 0}(t)\frac{r_0}{r} \tag{33a}$$

$$B_z = B_{z0}(t)\left(\frac{r_0}{r}\right)^n. \tag{33b}$$

At $t = 0$, the particle is assumed to be matched at $r = r_0$; hence (for a relativistic particle)

$$r_0 = \frac{mc^2}{e}\frac{\gamma(0)}{B_{z0}(0)}.$$

During acceleration, the particle is allowed to move its matched radius to $r(t)$,

satisfying

$$r(t) = \frac{mc^2}{e}\frac{\gamma(t)}{B_z(r(t), t)} = \frac{mc^2}{e}\frac{\gamma(t)}{B_{z0}(t)}\left[\frac{r(t)}{r_0}\right]^n, \tag{35}$$

or solving for $r(t)$,

$$r(t) = r_0\left[\frac{mc^2}{er_0}\frac{\gamma(t)}{B_{z0}(t)}\right]^{1/(1-n)}. \tag{36}$$

If $b =$ constant at $r = r(t)$ is required to fix the tune,

$$b = \frac{B_{\theta 0}(t)}{B_{z0}(t)}\left(\frac{r_0}{r(t)}\right)^{1-n} = \frac{er_0}{mc^2}\frac{B_{\theta 0}(t)}{\gamma(t)} = \text{constant}, \tag{37}$$

which implies that $B_{\theta 0}$ must increase synchronously with γ during acceleration. In the stellatron, the requirement for fixed tunes is that both b and ε be fixed separately. This demonstration that b cannot be fixed if the toroidal field is asynchronous with γ, therefore, applies to both the stellatron and the modified betatron. It is therefore not possible to fix the tunes in a modified betatron or stellatron with an asynchronous toroidal field that varies as r^{-1}.

Another possibility for controlling the growth of single-particle resonances may be to use nonlinear focusing fields to de-tune the resonance by making the tunes a function of the amplitude of the particle displacement. The Bessel functions which describe the $l = 0$ or $l = 2$ transverse fields, of course, already provide such a nonlinearity. The use of $l = 3$ fields in conjunction with a modified betatron or $l = 0, 2$ stellatron provides a high-shear nonlinear field which may be of benefit for the control of resonances.

Rapid acceleration of the beam may also provide a means of avoiding damage due to resonances by rapidly accelerating through them. Since the betatron wavelength depends on the particle energy, a stellatron with sufficient energy gain per pass will traverse a resonance before the beam can respond. This possibility has been addressed in the numerical calculation shown in Fig. 13. The first frame shows a stable electron orbit with $\gamma = 49$ and with no field error. In the next frame, a 2% integer field error ($n = 1$) is superimposed on the stellatron fields, and the unaccelerated electron trajectory is rapidly lost to the wall. The lower two frames show the effects of high-gain acceleration through the resonance. At a gain of 3 MeV/pass, the particle motion is essentially contained.

This result suggests that a high-gain stellatron accelerator, with rapidly varying fields, may be desirable. Such a device will not only be beneficial for the control of single-particle resonances, but also will have a shorter acceleration time than conventional betatrons, and will therefore be less sensitive to several collective instabilities. Resistive-wall instabilities, for example, are ineffective if the acceleration time is $\lesssim 100\ \mu$sec.

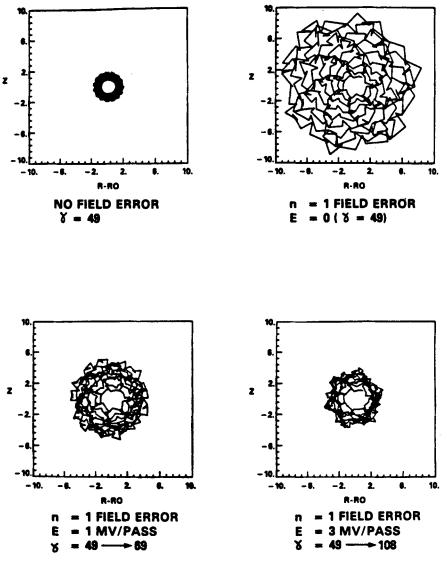

RESONANT ORBITS IN THE STELLATRON

FIGURE 13 Effect of acceleration through a resonance on transverse particle motion.

To allow field penetration in a fast stellatron, the vessel will have to be slotted, and acceleration will then occur primarily at the slots or gaps. The particles will therefore be unavoidably mismatched as they move between slots. The stellatron focusing can tolerate this mismatch, and is therefore compatible with this type of device.

V. INJECTION

Injection into a high-current cyclic accelerator is a challenge. The toroidal field lines that contain the space charge of the beam must be crossed or perturbed to get the beam in. A number of experiments have been carried out in similar geometries using inductive charging,[18,19,35] magnetic diverters,[46,47] and drift injection.[48] A self-synchronous scheme, using the current in the cathode shank to make a magnetic diverter, has been used to inject 50 percent of a 500-kV 20-kA 50-μsec beam into a racetrack torus.[47] These experiments by Gilad *et al.* and Benford *et al.* involve injecting the beam into neutral gas. A 450-keV 16-kA 25-μsec beam has been injected into a toroidal magnetic field in a hard vacuum[49] to obtain a trapped beam current of 300 A and a quiescent equilibrium for 20 μsec, which is approximately 3000 revolutions around the torus.

Recent experiments[50] have been carried out in which the torus is filled using a plasma gun. The spatial plasma-density profile is controlled by adjusting the direction of plasma injection or the timing between the gun firing and the

application of the pulse to the cathode. The plasma makes contact with both the cathode and the chamber wall. When the cathode is pulsed negatively, a double-layer plasma sheath appears, and the electrons of the cathode plasma are accelerated in the sheath and ejected into the plasma. With a 1.2-MV 80-μsec pulse, a current of 50 to 80 kA can be injected into the plasma. When the ring radius is held constant, the 40-kA ring decays to approximately half of its value in 400 μsec. When the ring is compressed, the 25-kA ring current increases to 50 kA and is contained for about 4 msec.[57]

Recently an axial pinch scheme has been proposed for injecting electrons across magnetic field lines into the NRL modified betatron.[52]

None of the prior experience has established a widely accepted solution to the injection problem. There are, nevertheless, several features of the stellatron field configuration that may be important from the standpoint of designing an injection scheme. The present discussion will be limited to the $l = 2$ stellatron.

The stellatron field has a separatrix within which the magnetic surfaces are closed and beyond which field lines run to the outside world. Injection along magnetic field lines can be used to place a beam just outside the separatrix. A fast-rising coil may be used locally to slip the separatrix over the beam, thus trapping it. Since the separatrix is a null field, it can be moved through the beam.

The rotational transform of the particle orbits due to the helical fields can be utilized to move the beam electrons away from an internal injector. Electrons can be forced to miss the injector for many revolutions of the accelerator. Figure 14 shows a beam injected at $\Delta r = 8$ cm, $\Delta z = 0$ moving in the toroidal direction with no transverse motion. The beam is injected with $I = 10$ kA, $\gamma = 7$ into fields,

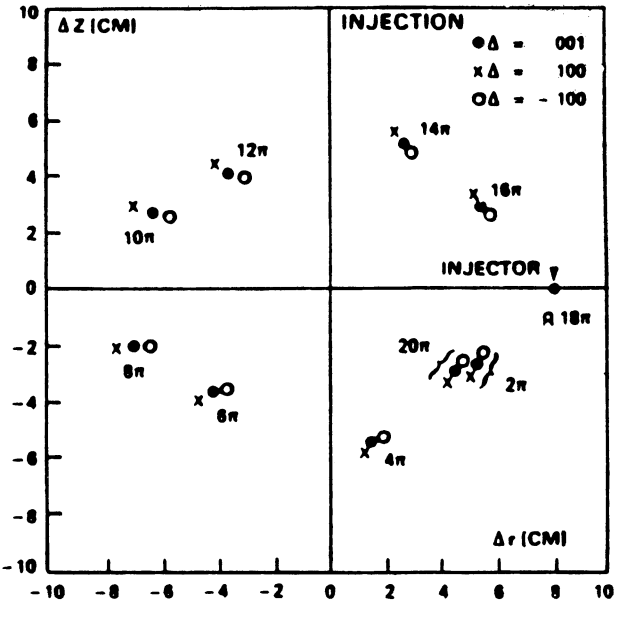

FIGURE 14 Location of beam center after injection.

$B_{\theta 0} = 5$ kG, $\varepsilon = 0.5$, $B_{z0} = 118$ G, $n = 0.5$. The analytical formalism developed in Section 2 is used to track the beam center around the torus. The points marked 2π, 4π, $6\pi, \ldots$ on the figure represent the location of the beam center after completing $1, 2, 3, \ldots$ transits of the torus. Approximately nine revolutions (200 μsec) are required to bring the beam electrons back to the vicinity of the injector. The open circles, filled circles and x's on the figure represent the injection of beams having $\Delta\gamma/\gamma_0 = 0.1\%$ mismatch, and $\pm 10\%$ mismatch. The injection dynamics are very insensitive to this mismatch. During the approximately 200ns required for the beam to return to the injector, the focusing fields must be changed to trap the electrons. A small change of the helical field (e.g., variation of ε) during injection may be effective in trapping the beam.

VI. DISCUSSION OF EARLIER WORK

During the course of this work, a number of people have pointed out related unpublished work. In particular, a report on a plasma betatron that has tested a field configuration similar to the $l = 2$ stellatron has been recently brought to our attention.[53] The device consists of a betatron field together with toroidal, helical, and multipole field capability to study plasma containment configurations. The addition of a betatron field to the system is motivated by the production of runaway electrons observed in the ORMAK tokamak.[15] Acceleration is obtained by changing the flux in a central solenoid. The field at the equilibrium orbit from this solenoid is nulled to zero by compensating coils. A separate set of programmable vertical-field coils is used to provide the equilibrium. One of the reasons given for driving the vertical field coils separately is that the 2-to-1 flux rule is not valid for currents comparable to the Alfven current,[53] due to self-field effects.

The equilibrium beam production in a plasma betatron is complex. The energetic beam is composed of runaway[54] electrons. The current due to those electrons that do not run away is generally an order of magnitude higher than the runaways. The vertical field is set to provide an equilibrium for the plasma currents. The interpretation of the limiting energy of the plasma betatron in terms of the work presented in this paper is as follows. The plasma currents provide a rotational tranform that contains the high-energy particles. This transform can be converted into an effective energy bandwidth. As the energy of the particles increases, the mismatch between the parallel energy and vertical field increases. Since the vertical field must be programmed to maintain the plasma-current equilibrium, this mismatch will grow until the beam orbit size exceeds the dimensions of the chamber. Hence, the maximum energy in a plasma betatron will be the bandwidth provided by the plasma current and the energy of the equilibrium orbit due to the vertical field. Runaway electrons with energies of a few megavolts are not unusual in tokamaks, and a 1.5-MeV beam has been produced in a plasma betatron.[55] In the Livermore plasma-betatron experiment, the beam energy is several hundred kilovolts and the beam current is about 10 A. The plasma current is 10 kA.

The complexity of forming a beam from runaways makes the interpretation of

the Livermore results ambiguous. With the helical field, the observed runaway production is approximately 10 times more intense and occurs at a much lower pressure, indicating that the helical field configuration confines single particles, but that an azimuthal current is necessary to continue the runaways in the absence of a helical field. Without the helical field, the x-ray burst from the beam hitting the wall occurs at approximately 200 μsec. With the helical field, the x-ray burst occurs at 800 μsec. The observed energy is only 200 keV, however, which is only a fraction of what should be obtained if acceleration occurs throughout the pulse.

R. Moir has sent results from interesting work that used an $\mathbf{E}\times\mathbf{B}$ injector in a racetrack geometry.[56] The trajectories of an $l=2$ helical field combined with a vertical field on one of the bends of a racetrack geometry is studied at low energies. Resonant and nonresonant diffusion of very low current electron beams has been studied. The beam makes 100 transits when the stellerator winding is on, which is about a factor of 5 better than without the stellarator windings.

The stability plane for continuously rotated magnetic quadrupoles in a linear transport system has been obtained previously.[57] A stability plane similar to Fig. 4 results.

In a series of early experiments[58] at the Naval Research Laboratory, D.C., de Packh has combined a betatron and solenoidal lens fields. The excessive currents required to raise the solenoid lens synchronously so as not to cross resonances causes excessive heating. He has also tested a combination betatron and air-core quadrupole system that can be programmed so that no resonance are crossed. With a 55 keV injection voltage he has injected and accelerated a 1/2 amp beam to 2 MeV.

J. D. Lawson has pointed out some early work on particle orbits in a betatron with a toroidal magnetic field.[59] The coupling between the radial and vertical betatron oscillations due to the toroidal field is examined. This work has been motivated by some experiments in which the addition of an 8 gauss toroidal magnetic field to a conventional betatron reduces the output by 75%, largely because the injected electrons follow the toroidal field lines and intercepted the injector structure after one revolution.

In recent experiments at Cornell University[60] an electron ring, confined in a cold, partially ionized hydrogen plasma has been transported into a modified betatron field configuration and accelerated. The energy of the beam is increased from 1.1 to 3.3 MeV. Although there is no direct evidence of instabilities, the ring current decreases from 3 kA to 1.5 kA during the acceleration.

Recently, a periodic magnetic-focusing system for a high-current cyclic system has been suggested.[61] The toroidal field consists of a series of magnetic cusps. The paraxial equation for this configuration may be obtained from Eq. (20) taking $b\to\infty$ and $\varepsilon\to 0$ with $b\varepsilon$ fixed. Injection can take place on the open field lines and the nonlinear focusing of the cusp may give a sufficient tune shift to detune the single-particle resonances.

VII. SUMMARY

The addition of continuous strong focusing fields to a betatron or modified betatron leads to a new configuration that has a large tolerance to mismatch

between the particle energy and the vertical magnetic field, thereby relaxing both mechanical and electrical design requirements on the accelerator and the injector. The allowed mismatch bandwidth obtained by strong focusing is especially attractive for high-current accelerators, and is compatible with operation at high energy gain per pass.

Strong focusing also offers the advantage of introducing a threshold, γ_T, for the onset of the negative mass instability. For $\gamma < \gamma_T$, there is no negative-mass instability. The threshold is $\gamma_T \approx 13$ for typical stellatron parameters.[40,41] The addition of stellarator windings to a betatron has not yet been analyzed in detail for its effect on collective instabilities. Other issues which are as yet unresolved include the evaluation of methods for avoiding orbital resonances and the demonstration of a beam injection technique.

The strong focusing associated with the stellatron allows a configuration to be designed with $n_s \gg 1/2$ at injection which will operate without passing through a disruptive diamagnetic-to-paramagnetic equilibrium transition[26,27] during acceleration. The modified betatron, on the other hand, suffers an instantaneous loss of momentum compaction as n_s passes through the value, 1/2, during acceleration.

Of the various l-number stellatrons, only the $l=0$ and $l=2$ configurations provide a finite transverse field gradient at the beam axis. Both configurations allow a large mismatch between the average beam energy and the equilibrium beam energy for the applied vertical field. Both are also relatively insensitive to the vertical field index. The $l=0$ system appears easier to construct, but stability during acceleration requires the use of a large number of field periods, i.e. $m \geq b$. The $l=2$ configuration, on the other hand, requires a more complicated (quadrupole) field, but does not require a large number of field periods for stable operation; the field can be generated using modular coils.[62,63]

An objective of this study has been to describe a multi-kiloampere cyclic electron accelerator concept which is compatible with injectors based on Marx pulseline technology. Such injectors are limited to electron energy of a few MeV, and the accelerator must therefore tolerate significant beam self-fields at injection. These fields can lead to substantial beam emittance as well as beam mismatch with the vertical magnetic field. In addition, the Marx pulseline technology itself is limited in the voltage ripple and the shot-to-shot voltage reproducibility that can be achieved at reasonable cost. The accelerator must be able to tolerate such uncertainties in the injected beam parameters on each shot. The stellatron configurations described here have a large tolerance both to beam emittance and to beam mismatch, which makes this concept attractive for handling high currents and for mating to a Marx pulseline injector.

As this paper was being completed, encouraging experimental results from a group at the University of California at Irvine were reported to us.[66] A 200-A beam has been accelerated to 2 MeV in a small $l=2$ stellatron device; smaller currents have been accelerated to 4 MeV in the same experiment.

VIII. ACKNOWLEDGEMENTS

We have profited from discussions with many people during the course of this work, among them D. W. Kerst, A. E. Robson and members of the Advanced

Accelerator Project in the NRL Plasma Physics Division. We particularly appreciate the encouragement of T. Coffey.

This work has been supported by the Naval Research Laboratory. One of us (AM) has been supported under Contract Number N00173-80-C-0512, and one of us (DC) has been supported under Contract Number N00014-83-C-2157 with the Naval Research Laboratory.

REFERENCES

1. K. R. Prestwich, D. E. Hasti, R. B. Miller and A. W. Sharpe, *IEEE Trans. Nucl. Sci.* **NS-30,** 3155 (1983).
2. G. J. Caporaso *et al.*, Proc. 5th Intl. Top. Conf. on High-Energy Electron and Ion Beam Research and Technology (San Francisco, CA, 1983).
3. J. E. Leiss, N. J. Norris and M. A. Wilson, *Part. Accel.* **10,** 223 (1980).
4. B. Kulke, D. S. Ravenscroft and G. E. Vogtlin, *IEEE Trans. Nucl. Sci.* **NS-28,** 2882 (1982).
5. R. B. Miller *et al.*, *IEEE Trans. Nucl. Sci.* **NS-28,** 3343 (1981).
6. R. Avery *et al.*, *IEEE Trans. Nucl. Sci.* **NS-18,** 479 (1971).
7. D. W. Kerst, *Phys. Rev.* **58,** 841 (1940).
8. D. W. Kerst, G. D. Adams, H. W. Koch and C. S. Robinson, *Phys. Rev.* **78,** 297 (1950).
9. A. I. Pavlovskii, D. G. Kuleshov, A. I. Gerasimov, A. P. Klementev, V. D. Kuzemtsov, V. A. Tananakin and A. D. Turasov, *Sov. Phys. Tech. Phys.* **22,** 218 (1977).
10. J. M. Peterson, "Betatrons with Kiloampere Beams," LBL reprint, LBL 15206 (1982); Proc. 7th Conf. on Applications of Accelerators in Research and Industry (Denton, Texas, 1982).
11. K. R. Symon, D. W. Kerst, L. W. Jones, L. J. Laslett and K. M. Terwilliger, *Phys. Rev.* **103,** 1837 (1956).
12. L. A. Ferrari and K. C. Rogers, *Phys. Fluids* **10,** 1319 (1967); J. G. Linhart, Proc. 4th Intl. Conf. on Ionized Phenomena in Gases (North Holland Publ. Co., 1960), p. 981.
13. N. C. Christofilos, unpublished. (1950).
14. E. Courant, N. S. Livingston and H. Snyder, *Phys. Rev.* **88,** 1190 (1952).
15. D. A. Spong, J. F. Clarke and J. A. Rome, "Relativistic Electron Production in the Ormak Device", ORNL-TM-4120 (1973).
16. W. Bernstein, F. F. Chen, M. A. Head and A. Z. Kramz, *Phys. Fluids* **5,** 430 (1958).
17. G. S. Janes, R. H. Levy, H. A. Bethe, and B. T. Feld, *Phys. Rev. Lett.* **145,** 925 (1966), J. D. Daugherty, J. E. Eninger and G. S. Janes, *Phys. Fluids* **12,** 2677 (1969).
18. G. S. Janes, *Phys. Rev. Lett.* **15,** 135 (1965).
19. W. Clark, P. Korn, A. Mondelli and N. Rostoker, *Phys. Rev. Lett.* **37,** 592 (1976).
20. N. Rostoker, *Part. Accel.* **5,** 93 (1973).
21. P. Sprangle and C. A. Kapetanakos, *J. Appl. Phys.* **49,** 1 (1978).
22. N. Rostoker, *Comments Plasma Phys. Controlled Fusion* **6,** 91 (1980).
23. P. Sprangle, C. A. Kapetanakos, and S. J. Marsh, in Proceedings of the International Topical Conference on High-Power Electron and Ion Beam Research and Technology, Palaiseau, France, 1981, p. 803.
24. C. A. Kapetanakos, P. Sprangle and S. J. March, *Phys. Rev. Lett.* **49,** 741 (1982); C. A. Kapetanakos, P. Sprangle, D. P. Chernin, S. J. Marsh and I. Haber, *Phys. Fluids* **26,** 1634 (1983).
25. P. Sprangle and J. Vomvoridis, Naval Research Laboratory Report 4688 (1982).
26. D. P. Chernin and P. Sprangle, *Part. Accel.* **12,** 85 (1982); *Part. Accel.* **12,** 101 (1982).
27. John M. Finn and Wallace M. Manheimer, *Phys. Fluids* **26,** 3400 (1983); Wallace M. Manheimer and John M. Finn, *Part. Accel.* **14,** 29 (1983).
28. Wallace M. Manheimer, *Part. Accel.* **13,** 209 (1983).
29. R. C. Davidson and H. S. Uhm, *Phys. Fluids* **25,** 2089 (1982).
30. T. P. Hughes, M. M. Campbell and B. B. Godfrey, *IEEE Trans. Nucl. Sci.* **NS-30,** 2528 (1983).
31. G. Barak, D. Chernin, A. Fisher, H. Ishizuka and N. Rostoker, "High Current Betatron," Proc. of

the 4th Int'l. Conf. on High-Power Electron and Ion Beam Research and Technology (Palaiseau, France, June 29–July 3 1981) Vol. II, pp. 795ff.
32. G. Barak and N. Rostoker, *Phys. Fluids* **26,** 856 (1983).
33. G. Roberts and N. Rostoker "Analysis of Modified Betatron with Adiabatic Particle Dynamics," Proc. of the 5th Intl. Conf. on High Power Electron and Ion Beam Research and Technology (San Francisco, California, 1983).
34. N. Rostoker, "High Current Betatron Experiments and Theory," Proc. of the 5th Intl. Conf. on High Power Electron and Ion Beam Research and Technology (San Francisco, California, 1983).
35. B. Mandelbaum, H. Ishizuka, A. Fisher and N. Rostoker, "Behavior of Electron Beam in a High Current Betatron," Proc. of the 5th Intl. Conf. on High Power Electron and Ion Beam Research and Technology, (San Francisco, California, 1983).
36. M. A. D. Wilson, *IEEE Trans. on Nucl. Sci.* **NS-28,** 3340 (1981).
37. C. W. Roberson, *IEEE Trans. on Nucl. Sci.* **NS-28,** 3433 (1981).
38. A. A. Mondelli and C. W. Roberson, "Energy Scaling Laws for the Racetrack Induction Accelerator," NRL Memorandum Report No. 5008 (1982), to be published in Particle Accelerators; "A High-Current Induction Accelerator" *IEEE Trans. on Nucl. Sci.* **NS-30,** 3212 (1983).
39. K. M. Young, *Plasma Physics* **16,** 119 (1974).
40. C. W. Roberson, A. A. Mondelli and D. Chernin; *Phys. Rev. Lett.* **50,** 507 (1983).
41. C. W. Roberson, A. A. Mondelli and D. Chernin; "The Stellatron—A Strong Focusing High Current Betatron" *IEEE Trans. Nucl.* **NS-30,** 3162 (1983).
42. A. A. Mondelli, D. Chernin and C. W. Roberson, "The Stellatron Accelerator," Proc. of the 5th Intl. Conf. on High Power Electron and Ion Beam Research and Technology (San Francisco, California, 1983).
43. D. Chernin, A. A. Mondelli and C. W. Roberson, *Phys. Fluids* **27,** 2378 (1984).
44. W. Magnus and S. Winkler, *Hill's Equation,* Dover Publications, Inc., New York, 1979.
45. I. S. Danilkin, in *Stellarators*; *Proc. of the P. N. Lebedev Physics Inst.*, D. V. Skobel'tsyn, ed. (Consultants Bureau, New York, 1979), Vol. 65, pp. 23 ff.
46. D. F. Brower, B. R. Kusse and G. D. Meixel, Jr., *IEEE Trans. on Plasma Sci.* **PS-2,** 193 (1974).
47. P. Gilad, B. R. Kusse and T. R. Lockner, *Phys. Rev. Lett.* **33,** 1275 (1974).
48. J. Benford *et al.*, *Phys. Rev. Lett.* **31,** 346 (1973). J. Benford, J. Guillory and C. Stallings, *J. Appl. Phys.* **45,** 1657 (1974); J. Benford, B. Ecker and V. Bailey, *Phys. Rev. Lett.* **33,** 574 (1975).
49. A. Mohri, M. Masuzaki, T. Tsuzuki and K. Ikuta, *Phys. Rev. Lett.* **34,** 574 (1975).
50. A. Mohri, K. Narihara, Y. Tomita, T. Tsuzuki, M. Hasegawa and K. Ikuta, Plasma Physics and Controlled Nuclear Fusion Research (Proc. 8th Int. Conf. Brussels, 1980) Vol. 1, IAEA, Vienna (1981) 511.
51. A. Mohri, K. Narihara, Y. Tomita, M. Hasegawa, T. Tsuzuki and T. Kobata, "REB Injected Toroidal Plasma," International Conference on Plasma Physics, Goteborg, Sweden, (1982).
52. F. Mako, W. Manheimer, C. A. Kapetanakos, D. Chernin and F. Sandel, "External Injection into a High Current Modified Betatron Accelertaor," NRL Memorandum Report 5196 (1983).
53. T. J. Fessenden, C. W. Hartman and R. H. Munger, "Preliminary Study of the Acceleration of Electrons in a Plasma Betatron," UCRL-78016 (1976).
54. H. Dreicer, *Phys. Rev.* **117,** 329 (1960).
55. J. Dress and W. Paul, *Z. Phys.* **180,** 380 (1964).
56. Ralph W. Moir, "Experimental Investigations of Nonadiabatic Scattering of Charged Particles in a Toroidal Magnetic Field," Ph.D. Thesis, Massachusetts Institute of Technology (1967).
57. R. L. Gluckstern, Proc. of Linear Accelerator Conference, 245 (1979).
58. D. C. dePackh, NRL Quarterly on Nuc. Sci. and Tech, 31 (1958); NRL Quarterly on Nuc. Sci. and Tech., 32 (1961); Bulletin of the American Physical Society, Series II, 5: 225 (1960).
59. W. Walkinshaw and K. Wyllie, TRE (Malvern) Maths Memo/58/WW, June 7 (1948). (Unpublished).
60. D. P. Taggart, M. R. Parker, H. J. Hopman and H. H. Fleishmann, "Betatron Acceleration of Kiloampere Electron Rings in RECE-Christa" *IEEE Trans. Nucl. Sci.* **NS-30,** 3165 (1983).
61. S. Humphries, Jr. and D. M. Woodall, *Bull. Am. Phys. Soc.* **28,** 1054 (1983).

62. M. A. Ivanorskii *et al.*, 'The Tor-2 Stellarator" in *Stellarators*, Proc. of the P. N. Lebedev Physics Inst., D. V. Skobeltsyn, editor (Consultants Bureau, New York, c. 1974), vol. 65, pp. 61 ff.
63. T. K. Chu *et al.*, "Modular Coils: A Promising Toroidal Reactor Coil System", Princeton Plasma Physics Laboratory Report PPPL-1796 (April, 1981).
64. M. Reiser, *Part. Accel.* **8,** 167 (1978).
65. Yu. L. Klimontovich, *Zhur. Eksptl. Teoret. Fiz.* **33,** 982 (1957) [*Sov. Phys. JETP* **6,** 753 (1958)]. See also, e.g. S. Ichimaru *Basic Principles of Plasma Physics: A Statistical Approach* (W. A. Benjamin; Reading, MA.; 1973).
66. N. Rostoker, private communication.

APPENDIX

This Appendix discusses the method of averaging Eqs. (6a–6c) over particle initial conditions so as to find separate equations for the particle position $(r_1(t), z_1(t))$—"Lagrangian" variables, dependent on the individual particle's initial position and momentum, and for the location of the beam center, $(\Delta r(\theta, t), \Delta z(\theta, t))$—"Eulerian" or field variables dependent only on time t and the observation point θ. The radial coordinate is treated here; identical expressions hold for z.

The distribution function may be defined in complete generality in "Klimontovich" form[65]

$$f(r, \theta, z, p_r, p_\theta, p_z; t) = \int \mathrm{d}^3 r^{(0)}\, \mathrm{d}^3 p^{(0)} f^{(0)}(\mathbf{r}^{(0)}, \mathbf{p}^{(0)}) \cdot \delta^{(3)}(\mathbf{r} - \tilde{\mathbf{r}}(\mathbf{r}^{(0)}, \mathbf{p}^{(0)}, t)) \cdot \delta^{(3)}(\mathbf{p} - \tilde{\mathbf{p}}(\mathbf{r}^{(0)}, \mathbf{p}^{(0)}, t)), \tag{A-1}$$

where $\mathbf{r}^{(0)}$ and $\mathbf{p}^{(0)}$ are the initial position and momentum of a particle, $\tilde{\mathbf{r}}$ and $\tilde{\mathbf{p}}$ are the solutions to the equations of motion for a particle of given initial position and momentum, and the integral extends over all initial conditions. At a given azimuth θ, then

$$\Delta r(\theta, t) = \frac{\int r\, \mathrm{d}r\, \mathrm{d}z\, \mathrm{d}^3 p (r - r_0) f(r, \theta, z, p_r, p_\theta, p_z; t)}{\int r\, \mathrm{d}r\, \mathrm{d}z\, \mathrm{d}^3 p f(r, \theta, z, p_r, p_\theta, p_z; t)}$$

$$= \frac{\int \mathrm{d}^3 r^{(0)}\, \mathrm{d}^3 p^{(0)} f^{(0)}(\mathbf{r}^{(0)}, \mathbf{p}^{(0)}) r_1\, \delta(\theta - \tilde{\theta})}{\int \mathrm{d}^3 r^{(0)}\, \mathrm{d}^3 p^{(0)} f^{(0)}(\mathbf{r}^{(0)}, \mathbf{p}^{(0)})\, \delta(\theta - \tilde{\theta})}$$

$$\equiv \langle r_1 \rangle, \tag{A-2}$$

where $r_1 = \tilde{r} - r_0$ and the arguments of r_1 and $\tilde{\theta}$ have been suppressed. Next consider the quantity $\langle \dot{r}_1 \rangle$ and relate it to derivatives of $\Delta r(\theta, t)$. Defining for convenience the operator $\hat{f}$ as

$$\hat{f}\phi = \int \mathrm{d}^3 r^{(0)}\, \mathrm{d}^3 p^{(0)} f^{(0)}(\mathbf{r}^{(0)}, \mathbf{p}^{(0)}) \phi(\mathbf{r}^{(0)}, \mathbf{p}^{(0)})$$

one finds

$$\begin{aligned}
\langle \dot{r}_1 \rangle &= \frac{\hat{f} \cdot \dfrac{\partial r_1}{\partial t}\, \delta(\theta - \tilde{\theta})}{\hat{f} \cdot \delta(\theta - \tilde{\theta})} \\
&= \frac{\dfrac{\partial}{\partial t}(\hat{f} \cdot r_1 \delta(\theta - \tilde{\theta})) - \hat{f} \cdot r_1 \dfrac{\partial}{\partial t}\delta(\theta - \tilde{\theta})}{\hat{f} \cdot \delta(\theta - \tilde{\theta})} \\
&= \frac{\dfrac{\partial}{\partial t}(\hat{f} \cdot r_1 \delta(\theta - \tilde{\theta})) + \dfrac{\partial}{\partial \theta}(\hat{f} \cdot r_1 \dot{\tilde{\theta}} \delta(\theta - \tilde{\theta}))}{\hat{f} \cdot \delta(\theta - \tilde{\theta})} \\
&= \frac{\partial}{\partial t}\left[\frac{\hat{f} \cdot r_1 \delta(\theta - \tilde{\theta})}{\hat{f} \cdot \delta(\theta - \tilde{\theta})}\right] + \frac{\partial}{\partial \theta}\left[\frac{\hat{f} \cdot r_1 \tilde{\theta} \delta(\theta - \tilde{\theta})}{\hat{f} \cdot \delta(\theta - \tilde{\theta})}\right] \\
&\quad - \frac{[(\hat{f} \cdot r_1 \delta(\theta - \tilde{\theta})) \cdot \dfrac{\partial}{\partial \theta} \hat{f} \cdot \dot{\tilde{\theta}} \delta(\theta - \tilde{\theta}) - (\hat{f} \cdot r_1 \dot{\tilde{\theta}} \delta(\theta - \tilde{\theta})) \cdot \dfrac{\partial}{\partial \theta} \hat{f} \cdot \delta(\theta - \tilde{\theta})}{[\hat{f} \cdot \delta(\theta - \tilde{\theta})]^2}
\end{aligned} \tag{A-3}$$

To this point, the expression for $\langle \dot{r}_1 \rangle$ is formally exact. To make further progress the linearization approximation is utilized in order to make the replacement $\dot{\tilde{\theta}}_0 \approx \dot{\theta}_0 \equiv \Omega_{z0}$. To linear order, then, from (A-3)

$$\langle \dot{r}_1 \rangle = \left(\frac{\partial}{\partial t} + \Omega_{z0} \frac{\partial}{\partial \theta}\right) \Delta r(\theta, t) \tag{A-4}$$

Similarly one may show, to the same order of approximation,

$$\langle \ddot{r}_1 \rangle = \left(\frac{\partial}{\partial t} + \Omega_{z0} \frac{\partial}{\partial \theta}\right)^2 \Delta r(\theta, t). \tag{A-5}$$

Equations (A-4, 5) and the corresponding equations for $\langle \dot{z}_1 \rangle$ and $\langle \ddot{z}_1 \rangle$ are used in the text to obtain (7a, b) from (6a, b).